Control of molecular excitation during the plasma generation of a femtosecond laser pulse

Quanjun Wang (王全军), Yanghua Zhang (张杨华), Zhenhao Wang (王贞浩), Jingjie Ding (丁晶洁), Zuoye Liu (刘作业)*, and Bitao Hu (胡碧涛)

School of Nuclear Science and Technology, Lanzhou University, Lanzhou 730000, China
**Corresponding author: zyl@lzu.edu.cn*

Received June 7, 2016; accepted August 26, 2016; posted online October 17, 2016

From a classical dynamic simulation, we find the kinetic energy of the electrons generated during laser plasma generation depends on the laser polarization and intensity. The electron kinetic energy reaches its maximum with a fixed laser intensity for circularly polarized laser pulse. The fluorescence spectra at 380.4 nm from N_2 and 391.3 nm from N_2^+ are measured; these are generated by both the direct excitation and electron collision excitation. The electron collision excitation is determined by the electron energy and reaches the maximal with a circularly polarized pulse.

OCIS codes: 020.2649, 020.2070, 300.6365.
doi: 10.3788/COL201614.110201.

The interaction of light and matter has been one of the most active and fundamental research fields in atomic physics for many years[1–13]. Laser filamentation in gaseous media is an important branch, exhibiting as a long, bright plasma channel[14–19]. Filamentation sets in when the intensity of such a laser beam exceeds the critical power $P_{\rm cr}$, i.e., the self-focusing induced by the Kerr effect prevails and leads to beam collapse, which is then stopped by the defocusing effect of the plasma generated by the multiphoton absorption of nitrogen and oxygen molecules. A dynamic balance between these opposite effects is then established, and the beam is able to maintain a very high intensity over long distances without significant defocusing. The excitation of nitrogen and oxygen molecules due to strong laser field leads to characteristic fluorescence radiation, based on which the laser-induced breakdown spectroscopy (LIBS) was developed and is now widely used in quantitative analyses of chemical elements[20,21].

Except for LIBS, few-cycle pulse generation, THz radiation, remote sensing of atmospheric pollution, light and discharge triggering, etc. are all unfolded from laser filamentations. Meanwhile, investigations into laser plasma generation dynamics were also performed to understand the excitation, the ionization, the process leading to fluorescence, and the plasma temperature, all of which depend on the intensity, the polarization, and number of external fields[22–24]. As is well known, the fluorescence spectra and the kinetic energies of free electrons born during laser filamentations change with the laser polarization[24,25]. However, the peak intensity inside a filament generated by an 800 nm laser pulse in air is clamped to 5×10^{13} W/cm^2[26], and the intensity dependence of the molecular excitation in a plasma generated by a femtosecond laser pulse is still an open question. A good understanding will help people interpret the fundamental phenomenon of laser plasma generation and develop its further applications, for instance, backward and forward lasing in air[22,27].

In the present work, how the laser intensity and polarization affect the molecular excitation during the plasma generation of a femtosecond laser pulse is studied. The electron energy spectrum generated by a strong laser field in air is calculated, and the result shows the free electron energy increases by tuning the laser polarization from linear to circular. With the increase of free electron energy, the electron collision excitation will affect laser plasma generation, exhibiting as the change of the proportion of different excited particles. To confirm this result, the fluorescence emission at 380.4 nm from N_2 ($C^3\Pi_u \rightarrow B^3\Pi_g$) and 391.3 nm from N_2^+ ($B^2\Sigma_{u^+} \rightarrow X^2\Sigma_{g^+}$) is measured with different laser polarizations, and it agrees well with the simulation.

When a femtosecond laser pulse interacts with air, N_2 and O_2 are ionized with the generation of free electrons. An adiabaticity parameter $\eta = (\varepsilon_i/2\varepsilon_{\rm quiv})^{\frac{1}{2}}$ is defined to determine the ionization method[28], where ε_i is the ionization potential (here, it is 15.6 eV for N_2) and $\varepsilon_{\rm quiv} = e^2E_0^2/4m_e\omega^2$ is the average quiver energy. e is the electron charge, m_e is the electron mass, E_0 is the peak laser field intensity, and ω is the laser frequency. When $\eta < 1$, tunneling ionization takes effect; otherwise, it is multiphoton ionization. By a simple calculation, the peak laser intensity $I_p = 1.4 \times 10^{14}$ W/cm^2 is the boundary of the two-ionization model for N_2. During the laser pulse duration, considering the time from t_0 to $t_0 + \Delta t$, $(\partial n_e/\partial t)_{t_0} \times \Delta t$ electrons will be liberated, where $n_e(t)$ denotes the electron density. $(\partial n_e/\partial t)_{t_0}$ can be calculated by ionization rate equations[29,30]. When the free electrons are liberated, they will be accelerated by the follow-up electric field. The electric field of laser pulse for the simulation is formulized as

$$\boldsymbol{E}(t) = \sqrt{\frac{8\pi\varepsilon_0}{c}I_p}\,\cos(\pi t/T)[\cos(\omega t+\phi)\boldsymbol{u}_x + \varepsilon\,\sin(\omega t+\phi)\boldsymbol{u}_y]\theta\left(\frac{T}{2}-|t|\right), \quad (1)$$

where ε_0, c, T, and θ are the vacuum permittivity, light speed, laser pulse duration (35 fs, in our case), and the Heaviside function. ε denotes the laser polarization. ϕ is an arbitrary carrier envelope phase, which is set as $\phi = 0$ in our case. The evolution of the transverse electron momentum can be described by the Newton equation. After the laser pulse, the transverse electron energy E_{kin}, produced at t_0, is

$$E_{\mathrm{kin}} = 2U_p \cos^2(\pi t_0/T)[1-(1-\varepsilon^2)\cos^2(\omega t_0)], \quad (2)$$

where $U_P = \frac{e^2 I_p}{2c\varepsilon_0 m_e \omega^2}$. As is well known, the kinetic energy of the free electrons in gaseous plasma generated by a strong laser field with linear and circular polarization is different[31,32]. By adjusting the coefficient ε from 0 to 1, the laser polarization is tuned from linear to circular.

The results in Figs. 1(a) and 1(b) show the calculated energy spectra of the free electrons generated by the external laser field of an intensity of 1.4×10^{14} W/cm^2 with different polarizations. With linear polarization, most electrons are left with energy less than 2.0 eV, because electrons experience an acceleration and deceleration process, while the maximum value of the electron energy distribution is around 16.0 eV in the case of circular polarization. Figures 1(c) and 1(d) show the simulated average energy of the liberated electrons as a function of the laser intensity in the range from 0.1×10^{14} to 2.4×10^{14} W/cm^2 with linear and circular polarizations. The electron kinetic energy increases with the laser intensity I_p. The average energy of the electrons generated by a linearly polarized laser pulse is much smaller than that of a circularly polarized laser pulse and does not exceed 2.0 eV at a laser intensity of 2.4×10^{14} W/cm^2, while that generated by a circularly polarized pulse can reach 22 eV. The average electron energy under a linear polarization pulse

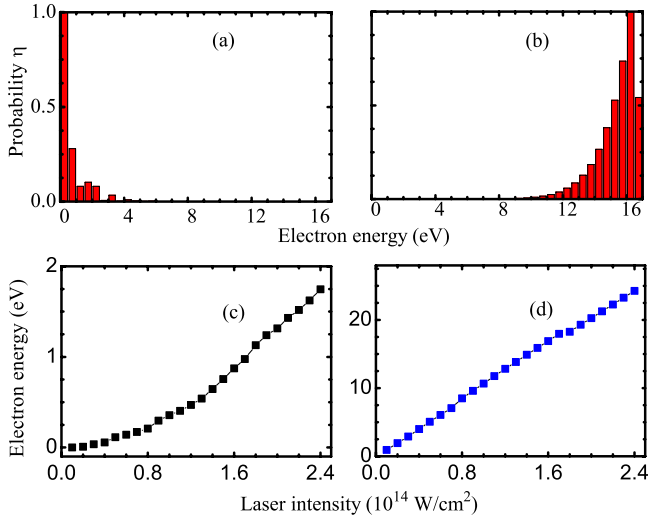

Fig. 1. Calculated energy distribution of free electrons in the case of (a) linearly ($\varepsilon = 0$) and (b) circularly ($\varepsilon = 1.0$) polarized laser pulses with an intensity of 1.4×10^{14} W/cm^2, and the average electron energy with varying laser intensities with (c) linear and (d) circular polarizations.

increases faster when the intensity is greater than 1.2×10^{14} W/cm^2, at which point, tunneling ionization almost supplants multiphoton ionization. By contrast, the average energy nearly increases linearly for circular laser polarization. Therefore, the polarization and intensity of the incident laser pulse hold the key to controlling the kinetic energy of the generated electrons, i.e., to controlling the collision excitation during the plasma generation process, as suggested by previous studies[24].

In order to test how the electron energy affects the laser plasma generation experimentally, we put our attention to the fluorescence emissions 380.4 nm from N_2 ($C^3\Pi_u \rightarrow B^3\Pi_g$) and 391.3 nm from N_2^+ ($B^2\Sigma_u^+ \rightarrow X^2\Sigma_g^+$) of laser-induced plasma, which are experimentally measurable. There are three different processes to get N_2 ($C^3\Pi_u$)[33–35]. One process is collision-assisted intersystem crossing from excited singlet states,

$$N_2 + mh\nu \rightarrow N_2^*, \qquad N_2^* + N_2 \rightarrow N_2(C^3\Pi_u) + N_2. \quad (3)$$

Another is

$$N_2^+ + 2N_2 \rightarrow N_4^+ + N_2, \qquad N_4^+ + e \rightarrow N_2(C^3\Pi_u) + N_2. \quad (4)$$

This is believed to be a minor contributor[35]. The collision process

$$N_2(X^1\Sigma_g^+) + e \rightarrow N_2(C^3\Pi_u) + e, \quad (5)$$

is believed to happen if the electron energy exceeds the energy threshold of 11 eV and the cross section reaches a maximum of 0.58 Å^2 at an electron energy of 14.5 eV[36]. The excited ionic $N_2^+(B^2\Sigma_u^+)$ is generated due to direct strong-field photon ionization of N_2 molecules[37], whose process can be written as

$$N_2 + mh\nu \rightarrow N_2^*, \qquad N_2^* + nh\nu \rightarrow N_2^+ + e. \quad (6)$$

With this process, the linear polarization is more efficient[37]. The electron collision ionization

$$N_2(X^1\Sigma_g^+) + e \rightarrow N_2^+(B^2\Sigma_u^+) + 2e, \quad (7)$$

will happen with a cross section of about 10^{-3} Å^2, when the electron energy reaches 27 eV[36]. The results in Figs. 1(c) and 1(d) indicate electron collision ionization can only happen if the laser intensity I_p exceeds 2.4×10^{14} W/cm^2, which is beyond the output limitation of our laser system for the experimental realization.

We measured the fluorescence spectral lines of 380.4 nm from N_2 and 391.3 nm from N_2^+ with femtosecond laser pulses of varying polarizations. In the experiment, a commercial Ti:Sapphire laser system operating at 1 kHz is employed to supply laser pulses with pulse duration of 40 fs, center wavelength of 800 nm. A single laser beam with a pulse energy up to 2.0 mJ was focused to generate a plasma by a lens with a focal length of $f = 100$ mm in

air. In the experiment, the plasma size is less than 1 cm, which does not exceed the Rayleigh length for our focused beam with a diameter of 160 μm, and so it is claimed to be a plasma rather than a filamentation. A quarter-wave plate ($\lambda/4$) was included in the beam path right before the lens. The initial polarization of laser pulse is linear, and the laser polarization can be adjusted from linear to elliptical and finally to circular by rotating the quarter-wave plate from 0° to 45°. A concave mirror was set at one side of the filament to collect and couple plasma fluorescence into a fiber-pigtailed spectrometer (McPherson 2061) with high resolution. The fiber head is put on a 3-axis stage, which is moved to find the maximum of the plasma fluorescence during the measurement. Due to the limitation of our laser system, the laser intensity I_p is limited to 2.4×10^{14} W/cm^2.

Figures 2(a) and 2(b) show the measured fluorescence spectrum for linearly and circularly polarized laser pulses with intensities of 0.1×10^{14} and 1.0×10^{14} W/cm^2, respectively. As our aim is the fluorescence emission generated by the decay of excited molecules and molecular ions, the continuum emission of the plasma due to free electrons impacting molecules and ions under the Coulomb force is subtracted artificially. With a low laser intensity of 0.1×10^{14} W/cm^2, the results in Fig. 2(a) show that the intensity of fluorescence emission of 391.3 nm for a linearly polarized pulse is stronger than that for the circularly polarized pulse, while there is no significant difference for the 380.4 nm emission generated by different polarization pulses. From the results displayed in Fig. 1(d), the average kinetic energy one electron can achieve is limited to about 1.85 eV under this laser intensity. With this value of energy, it is impossible to open the electron collision excitation channel. A linearly polarized laser pulse is more significant for N_2^+ generation than a circularly polarized pulse[37], as the linearly polarized pulse has a $\vec{u}_x$ component that is stronger than that of the circularly polarized pulse. The results illustrated in Fig. 2(b) show that the intensity of the 380.4 nm fluorescence emission generated by a circularly polarized pulse is higher than that generated by a linearly polarized pulse. The average kinetic energy one electron can achieve is around 11 eV, enabling the electron collision excitation channel shown by Eq. (5). Meanwhile, the 391.3 nm fluorescence emission generated by a circularly polarized pulse is still less than that generated by a linearly polarized pulse, i.e., the reaction channel displayed by Eq. (7) still has no obvious contribution to the 391.3 nm fluorescence emission. The dependence of the fluorescence emission at 380.4 and 391.3 nm generated by linearly and circularly polarized pulses on the laser intensity is illustrated in Figs. 2(c) and 2(d), respectively. The cross sections for the emission at 380.4 and 391.3 nm increase with the incident laser intensity for both linear and circular polarizations. Figure 2(c) shows directly that the electron collision excitation begins to affect the 380.4 nm fluorescence emission since $I_p = 0.5 \times 10^{14}$ W/cm^2. However, the density of molecular ion N_2^+ ($B^2\Sigma_u^+$) generated by a linearly polarized pulse is higher than that by circularly polarized pulse in our laser intensity range, as the kinetic energy one electron can achieved is less than 27 eV.

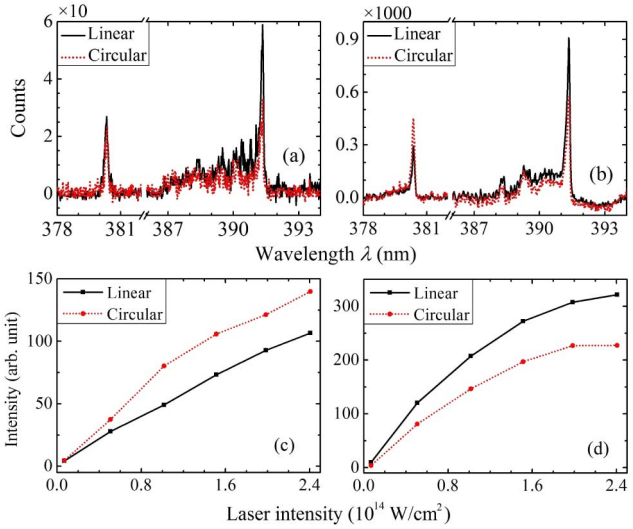

Fig. 2. Fluorescence emission due to the decay of excited molecule N_2 (380.4 nm) and molecular ion N_2^+ (391.3 nm) generated by linearly (black line) and circularly (red dot line) polarized laser pulses for intensities of (a) 0.1×10^{14} and (b) 1.0×10^{14} W/cm^2, respectively. (c) and (d) show the intensity of the fluorescence emission at 380.4 and 391.3 nm generated by linearly (square black solid line) and circularly (circle red dot line) polarized laser pulses with varying intensities, respectively.

Figure 3 displays the dependence of intensity ratio γ at 380.4 and 391.3 nm on the incident laser intensity. The ratio γ is defined as the fluorescence intensity generated by a circularly polarized pulse divides that generated by a linearly polarized pulse. With a low laser intensity of 0.1×10^{14} W/cm^2, the intensity ratio γ at 380.4 nm is less than 1.0, indicating the electron collision excitation has no contribution. The electron collision excitation (Eq. (5)) begins to affect the generation of excited molecule $N_2(C^3\Pi_u)$ at $I_p = 0.5 \times 10^{14}$ W/cm^2, and the intensity ratio γ at 380.4 nm is 1.4. The contribution from the electron collision excitation to the $N_2(C^3\Pi_u)$ generation first increases with the incident laser intensity until 1.0×10^{14} w/cm^2, then it begins to reduce until

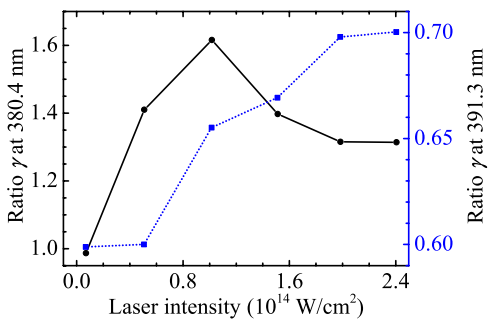

Fig. 3. Intensity ratio γ at 380.4 and 391.3 nm with varying laser intensities from $I_p = 0.1 \times 10^{14}$ to 2.4×10^{14} W/cm^2.

2.0×10^{14} W/cm^2, i.e., the cross section for the electron collision excitation of the electronic states of N_2 reaches its maximum at $I_p = 1.0 \times 10^{14}$. In the range from 2.0×10^{14} to 2.4×10^{14} W/cm^2, the ratio γ at 380.4 nm keeps constant, i.e., the electron collision excitation has a fixed contribution to the $N_2(C^3\Pi_u)$ generation. For the fluorescence emission at 391.3 nm, due to the decay of the excited molecular ion $N_2^+(B^2\Sigma_u^+)$, the electron collision ionization may contribute to the generation of $N_2^+(B^2\Sigma_u^+)$; however, the cross section is so low ($<10^{-3}$ Å^2) that it can be ignored within our intensity range[36]. The intensity ratio γ at 391.3 nm keeps increasing with the laser intensity, i.e., the cross section for the generation of $N_2^+(B^2\Sigma_u^+)$ due to the multiphoton absorption of a circularly polarized laser pulse increases faster than that of a linearly polarized laser pulse. From the tendency of γ at 391.3 nm and the results shown in Fig. 2(d), it can be predicted that the emission at 391.3 nm will reach saturation with higher intensities for both linear and circular polarizations.

Combined with a classical dynamic simulation, we study the excitation mechanism during femtosecond laser plasma generation by measuring the fluorescence at 380.4 nm from N_2 and 391.3 nm from N_2^+. The kinetic energy of the electron generated in the strong field can be manipulated by the laser polarization, which also exhibits a laser intensity dependence. For circularly polarized laser pulse, the electron kinetic energy reaches its maximal with a fixed laser intensity, resulting in the enhanced generation of excited N_2 due to the electron collision excitation. The study provides us with a way to control the excitation processes of laser plasma generation, which also benefits its applications, such as the backward and forward lasing.

This work was supported by the National Natural Science Foundation of China (Nos. 11504148 and 11135002) and the Fundamental Research Funds for the Central Universities (Nos. lzujbky-2015-269 and lzujbky-2015-242).

References

1. R. Mathies, C. Brito Cruz, W. Pollard, and C. Shank, Science **240**, 777 (1988).
2. M. Saes, C. Bressler, R. Abela, D. Grolimund, S. L. Johnson, P. A. Heimann, and M. Chergui, Phys. Rev. Lett. **90**, 047403 (2003).
3. T. M. Clarke, F. C. Jamieson, and J. R. Durrant, J. Phys. Chem. C **113**, 20934 (2009).
4. M. Chini, X. Wang, Y. Cheng, Y. Wu, D. Zhao, D. A. Telnov, S.-I. Chu, and Z. Chang, Sci. Rep. **3**, 1105 (2013).
5. A. Gandman, L. Rybak, and Z. Amitay, Phys. Rev. Lett. **113**, 043003 (2014).
6. C. Ott, A. Kaldun, P. Raith, K. Meyer, M. Laux, J. Evers, C. H. Keitel, C. H. Greene, and T. Pfeifer, Science **340**, 716 (2013).
7. Z. Liu, C. Ott, S. M. Cavaletto, Z. Harman, C. H. Keitel, and T. Pfeifer, New J. Phys. **16**, 093005 (2014).
8. Z. Liu, S. M. Cavaletto, C. Ott, K. Meyer, Y. Mi, Z. Harman, C. H. Keitel, and T. Pfeifer, Phys. Rev. Lett. **115**, 033003 (2015).
9. Z. Hao, J. Zhang, Y. Li, X. Lu, X. Yuan, Z. Zheng, Z. Wang, W. Ling, and Z. Wei, Appl. Phys. B **80**, 627 (2005).
10. W. Liu, Q. Luo, and S. L. Chin, Chin. Opt. Lett. **1**, 56 (2003).
11. Y. Chen, S. Yu, R. Sun, C. Gong, L. Hua, X. Lai, W. Quan, and X. Liu, Chin. Phys. Lett. **33**, 043301 (2016).
12. T. Zeng, H. Gao, X. Sun, and W. Liu, Chin. Opt. Lett. **13**, 070008 (2015).
13. K. Kaneshima, K. Takeuchi, N. Ishii, and J. Itatani, High Power Laser Sci. Eng. **4**, e17 (2016).
14. Z. Hao, J. Zhang, X. Lu, T. Xi, Y. Li, X. Yuan, Z. Zheng, Z. Wang, W. Ling, and Z. Wei, Opt. Lett. **14**, 773 (2006).
15. A. Couairon and A. Mysyrowicz, Phys. Rep. **441**, 47 (2007).
16. L. Berg, S. Skupin, R. Nuter, J. Kasparian, and J.-P. Wolf, Rep. Prog. Phys. **70**, 1663 (2007).
17. S. Yuan, S. L. Chin, and H. Zeng, Chin. Phys. B **24**, 014208 (2015).
18. H. Liang, H. Sun, Y. Liu, Y. Tian, J. Ju, C. Wang, and J. Liu, Chin. Opt. Lett. **13**, 033201 (2015).
19. Y. Wei, Y. Liu, T. Wang, N. Chen, J. Ju, Y. Liu, H. Sun, C. Wang, J. Liu, H. Lu, S. L. Chin, and R. Li, High Power Laser Sci. Eng. **4**, e8 (2016).
20. C. Pasquini, J. Cortez, L. Silva, and F. B. Gonzaga, J. Brazil. Chem. Soc. **18**, 463 (2007).
21. F. J. Fortes, J. Moros, P. Lucena, L. M. Cabalín, and J. J. Laserna, Anal. Chem. **85**, 640 (2012).
22. P. Ding, S. Mitryukovskiy, A. Houard, E. Oliva, A. Couairon, A. Mysyrowicz, and Y. Liu, Opt. Express **22**, 29964 (2014).
23. B. Hu, Z. Liu, L. Li, S. Sun, P. Ding, X. Liu, Q. Liu, Z. Guo, and B. Ding, Laser Phys. Lett. **10**, 075401 (2013).
24. S. Mitryukovskiy, Y. Liu, P. Ding, A. Houard, A. Couairon, and A. Mysyrowicz, Phys. Rev. Lett. **114**, 063003 (2015).
25. B. Zhou, A. Houard, Y. Liu, B. Prade, A. Mysyrowicz, A. Couairon, P. Mora, C. Smeenk, L. Arissian, and P. Corkum, Phys. Rev. Lett. **106**, 255002 (2011).
26. J. Kasparian, R. Sauerbrey, and S. L. Chin, Appl. Phys. B **71**, 877 (2000).
27. J. Yao, S. Jiang, W. Chu, B. Zeng, C. Wu, R. Lu, Z. Li, H. Xie, G. Li, C. Yu, Z. Wang, H. Jiang, Q. Gong, and Y. Cheng, Phys. Rev. Lett. **116**, 143007 (2016).
28. S. C. Rae and K. Burnett, J. Phys. B: At. Mol. Opt. Phys. **26**, 1509 (1993).
29. C. Ireland and C. G. Morgan, J. Phys. D **6**, 720 (1973).
30. S. L. Chin, Y. Liang, J. E. Decker, E. Jennifer, F. A. Ilkov, and M. V. Ammosov, J. Phys. B: At. Mol. Opt. Phys. **25**, L249 (1992).
31. P. Bucksbaum, M. Bashkansky, R. Freeman, T. McIlrath, and L. DiMauro, Phys. Rev. Lett. **56**, 2590 (1986).
32. P. B. Corkum, N. H. Burnett, and F. Brunel, Phys. Rev. Lett. **62**, 1259 (1989).
33. H. L. Xu, A. Azarm, J. Bernhardt, Y. Kamali, and S. L. Chin, Chem. Phys. **360**, 171 (2009).
34. H. L. Xu, Y. Cheng, S. L. Chin, and H. B. Sun, Laser Photon. Rev **9**, 275 (2015).
35. B. R. Arnold, S. D. Roberson, and P. M. Pellegrino, Chem. Phys. **405**, 9 (2012).
36. Y. Itilawa, J. Phys. Chem. Ref. Data **35**, 31 (2006).
37. A. Becker, A. D. Bandrauk, and S. L. Chin, Chem. Phys. Lett. **343**, 345 (2001).